DEVELOPMENT OF A COMPUTER CODE TO SIMULATE AEROSOL BEHAVIOR IN A VENTED CONTAINMENT

NUCLEAR REACTOR SAFETY

TECHNICAL NOTE

A. K. AHLUWALIA and A. M. C. CHAN *Ontario Hydro Research Division*
800 Kipling Avenue, Toronto, Ontario, Canada M8Z 5S4

Received February 14, 1990
Accepted for Publication May 23, 1990

A newly developed computer code, FONS-AERO, is used to simulate the flow parameters of a carrier gas and an aerosol in an idealized vented containment during a blowdown. The code is a transient, multidimensional turbulent flow code that can handle gas and aerosol flows simultaneously under various flow situations. Complicated boundary conditions can also be readily incorporated. Some initial results of aerosol distribution in the containment and sensitivity to aerosol types are presented.

INTRODUCTION

The behavior of nuclear aerosols in a power reactor containment is of great importance in assessing the radiological consequences of a severe accident in a nuclear power plant. Nuclear aerosols are encountered in many reactor accident scenarios. For example, in a loss-of-coolant accident, high-enthalpy coolant discharging into the containment from a ruptured pipe results in a high-velocity two-phase jet, which contains fine airborne liquid droplets with soluble fission products. For Canada deuterium uranium pressurized heavy water reactors with horizontal pressure tubes, a postulated accident scenario involves an end-fitting failure in which fuel bundles are ejected from a pressure tube. The fuel is damaged upon impact with containment structures and releases fission products in aerosol form into the containment atmosphere. In this accident scenario, high-enthalpy coolant also discharges from the failed pressure tube, forming a two-phase jet.

Fission products released in an accident are most hazardous while they remain airborne. Therefore, a major task of containment analysis is to calculate the behavior of aerosols inside the containment.

Many computer codes are available to predict the behavior of nuclear aerosols in the containment. A number of them were discussed and compared in Refs. 1 and 2. The governing equation solved is inevitably the integro-differential equation that describes the aerosol size distribution.[2] The codes differ mainly in the numerical solution technique used, the aerosol processes considered, and the detailed modeling of the containment. In general, the containment is represented only by one-dimensional control volumes and internal structures. Since most of the codes are not multidimensional, a detailed prediction of localized carrier gas and aerosol behavior is not possible.

A research program was initiated in the Ontario Hydro Research Division to develop a new computer code that can simultaneously calculate the local carrier gas thermal hydraulics and the aerosol dynamics in a multidimensional containment. As the thermal hydraulics of a flashing jet and the dynamic behavior of the aerosols are both exceedingly complex, it is necessary to approach the problem in phases. The first phase forms the basis of this paper. It focuses on the formulation and solution algorithm of the code using simplified physical models. Results using an idealized containment are also presented. The simplified models will then be refined further in subsequent phases.

MATHEMATICAL FORMULATION

The FONS-AERO code is a derivative of the FONS series of computer codes developed in at Ontario Hydro. The codes were used to simulate transient, laminar, or turbulent mixed and natural-convection problems in simple as well as complicated geometries. The formulation is based on the closure of the time-averaged momentum, mass continuity, and energy equations. Turbulence is modeled using a k-ϵ model. The flow is assumed to be incompressible, and buoyancy effects are accounted for by the Boussinesq approximation. Previous versions of the codes have been properly verified.[3-5] The new version, FONS-AERO, models the transport of aerosols in containment by incorporating into the computer code the aerosol concentration and velocity equations. The set of equations solved in FONS-AERO becomes as follows:

1. *Carrier gas*

Mass conservation equation:

$$\frac{\partial u}{\partial x} + \frac{\partial v}{\partial y} = 0 \tag{1}$$

Momentum conservation equations:

$$\frac{\partial u}{\partial t} + u\frac{\partial u}{\partial x} + v\frac{\partial u}{\partial y} = -\frac{1}{\rho}\frac{\partial p'}{\partial x} + \frac{1}{\rho}\frac{\partial}{\partial x}\left(\mu_E \frac{\partial u}{\partial x}\right) + \frac{1}{\rho}\frac{\partial}{\partial y}\left(\mu_E \frac{\partial u}{\partial y}\right) + \frac{1}{\rho}\frac{\partial}{\partial x}\left(\mu_E \frac{\partial u}{\partial x}\right) + \frac{1}{\rho}\frac{\partial}{\partial y}\left(\mu_E \frac{\partial v}{\partial x}\right) - \frac{2}{3}\frac{\partial k}{\partial x} \tag{2}$$

$$\frac{\partial v}{\partial t} + u\frac{\partial v}{\partial x} + v\frac{\partial v}{\partial y} = -\frac{1}{\rho}\frac{\partial p'}{\partial y} + \frac{1}{\rho}\frac{\partial}{\partial x}\left(\mu_E \frac{\partial v}{\partial x}\right) + \frac{1}{\rho}\frac{\partial}{\partial y}\left(\mu_E \frac{\partial v}{\partial y}\right) + \frac{1}{\rho}\frac{\partial}{\partial x}\left(\mu_E \frac{\partial u}{\partial y}\right) + \frac{1}{\rho}\frac{\partial}{\partial y}\left(\mu_E \frac{\partial v}{\partial y}\right) - \frac{2}{3}\frac{\partial k}{\partial y} + g\beta_T(T - T_R) + g\beta_C(C - C_R) , \tag{3}$$

where

$$\mu_E = \mu_L + \mu_T$$

and

$$\mu_T = C_\mu \rho \frac{k^2}{\epsilon} .$$

Energy conservation equation:

$$\frac{\partial T}{\partial t} + u\frac{\partial T}{\partial x} + v\frac{\partial T}{\partial y} = \frac{\partial}{\partial x}\left(\alpha_E \frac{\partial T}{\partial x}\right) + \frac{\partial}{\partial y}\left(\alpha_E \frac{\partial T}{\partial y}\right) , \tag{4}$$

where

$$\alpha_E = \alpha_L + \alpha_T = \mu_L/\rho Pr_L + \mu_T/\rho Pr_T$$

and

$$Pr_L = \frac{\mu_L C_P}{\gamma} .$$

Turbulent kinetic energy equation:

$$\frac{\partial k}{\partial t} + u\frac{\partial k}{\partial x} + v\frac{\partial k}{\partial y} = \frac{1}{\rho}\frac{\partial}{\partial x}\left(\frac{\mu_E}{\sigma_k}\frac{\partial k}{\partial x}\right) + \frac{1}{\rho}\frac{\partial}{\partial y}\left(\frac{\mu_E}{\sigma_k}\frac{\partial k}{\partial y}\right) + G - \epsilon - \beta_T g \frac{\mu_T}{\rho Pr_T}\frac{\partial T}{\partial y} - \beta_C g \frac{\mu_T}{\rho Sc_T}\frac{\partial C}{\partial y} . \tag{5}$$

Turbulent kinetic energy dissipation equation:

$$\frac{\partial \epsilon}{\partial t} + u\frac{\partial \epsilon}{\partial x} + v\frac{\partial \epsilon}{\partial y} = \frac{1}{\rho}\frac{\partial}{\partial x}\left(\frac{\mu_E}{\sigma_\epsilon}\frac{\partial \epsilon}{\partial x}\right) + \frac{1}{\rho}\frac{\partial}{\partial y}\left(\frac{\mu_E}{\sigma_\epsilon}\frac{\partial \epsilon}{\partial y}\right) + C_1\frac{\epsilon}{k}G - C_2\frac{\epsilon^2}{k} , \tag{6}$$

where G in Eqs. (5) and (6) is given by

$$G = \frac{\mu_T}{\rho}\left[2\left(\frac{\partial u}{\partial x}\right)^2 + 2\left(\frac{\partial v}{\partial y}\right)^2 + \left(\frac{\partial u}{\partial y} + \frac{\partial v}{\partial x}\right)^2\right] . \tag{7}$$

The values used for the different empirical constants in the turbulence equations are listed in Table I.

2. *Aerosol*

Mass conservation equation:

$$\frac{\partial C}{\partial t} + U_p\frac{\partial C}{\partial x} + V_p\frac{\partial C}{\partial y} = \frac{\partial}{\partial x}\left(D_E\frac{\partial C}{\partial x}\right) + \frac{\partial}{\partial y}\left(D_E\frac{\partial C}{\partial y}\right) - \bar{R} + \bar{S} , \tag{8}$$

where

$$D_E = D_L + D_T = \mu_L/\rho Sc_L + \mu_T/\rho Sc_T$$

$$Sc_L = \mu_L/\rho D_L$$

$\bar{R}$ = removal rate

$\bar{S}$ = source term.

Velocity equations:

$$\frac{4}{3}\pi R^3\rho_p\frac{\partial U_p}{\partial t} = 6\pi\mu_e R(U_p - u) + \frac{4}{3}\pi R^3\rho\frac{\partial u}{\partial t} + \frac{2}{3}\pi R^3\rho\left(\frac{\partial u}{\partial t} - \frac{\partial U_p}{\partial t}\right) + F_x \tag{9}$$

and

$$\frac{4}{3}\pi R^3\rho_p\frac{\partial V_p}{\partial t} = 6\pi\mu_e R(V_p - v) + \frac{4}{3}\pi R^3\rho\frac{\partial v}{\partial t} + \frac{2}{3}\pi R^3\rho\left(\frac{\partial v}{\partial t} - \frac{\partial V_p}{\partial t}\right) + F_y . \tag{10}$$

Equations (9) and (10) were obtained by balancing the forces acting on a particle in motion.[6] The first term on the right side is the viscous resistance given by Stokes' law. The second term is due to the pressure gradient in the carrier gas surrounding the particle. The third term denotes the force required to accelerate the apparent mass of the particle relative to the carrier gas. The last term represents external force fields that are considered insignificant in the present phase of the development.

Equations (8), (9), and (10) describe the dynamics of an aerosol of a given size. If more than one aerosol group is considered, the set of equations [Eqs. (8), (9), and (10)] will be repeated accordingly. Note that the aerosol is assumed to be carried along by and exerts no influence on the continuous phase.

Furthermore, no coagulation of the aerosol is assumed.

TABLE I

Values Used for Different Empirical Constants in Turbulence Equations

C_1	C_2	σ_k	σ_ϵ	C_μ	Sc_T	Pr_T
1.44	1.92	1.0	1.3	0.09	1.0	1.0

This assumption is true when the aerosol number concentration is low (on the order of 10^9 particle/m^3 or less).

NUMERICAL TECHNIQUE

The set of conservation equations is solved by the finite difference method described in detail in Ref. 3. The technique uses the primitive parameters, i.e., pressure and velocities, as dependent variables instead of vorticity and stream function. The finite difference mesh consists of rectangular control volume cells. A staggered grid is used in which velocities are defined at cell boundaries, whereas other dependent variables are defined at cell centers. The solution technique is explicit and employs the pressure correction concept.[7] The flow velocities are calculated explicitly from the momentum equations, first using previous time step values. The new velocity field is then adjusted iteratively to satisfy the mass conservation equation by adjusting the computation cell pressures. When the new converged velocity field is obtained, it is used to compute the fluid temperature, turbulence, and aerosol velocities and concentrations. The new set of dependent variables is then used for the next time step calculations.

Boundary conditions are applied by imposing appropriate velocities, temperatures, and aerosol properties on the boundary cells. For the turbulence quantities, the wall function method[8] is used.

Numerical stability is obtained if the fluid is not permitted to cross more than one cell in one time step, i.e., the Courant number must be <1. This can be achieved by limiting the time step size used. In the FONS codes, the time step size is optimized at each time step to ensure stability and efficiency.

Although the conservation equations are finite differenced and solved in two-dimensional rectangular coordinates to save computation time and costs, the code can be easily extended to model three-dimensional flows.

Physical Model

An idealized containment was used to test the computer code and to investigate the effects of carrier gas flow on aerosol transport. Details of the containment are given in Fig. 1. It consists of a two-dimensional rectangular vessel (5 × 2 m) with a 0.2-m vent at the top. A blowdown nozzle is located 0.7 m above the vessel floor and protrudes 0.5 m into the vessel. An impingement plate is used to simulate a wall or other obstruction. The distance L between the blowdown nozzle and the plate can be varied.

Calculations were performed with a 32 × 30 mesh. Variable mesh sizes were used to better resolve the flow field near the walls, the jet, and the vent. The following assumptions were made:

1. The vessel is well insulated. It is filled with stagnant steam at saturation before the blowdown is initiated.

2. Single-phase steam at saturation is discharged into the vessel during blowdown.

3. A monodisperse spherical aerosol at steam temperature is produced by an aerosol generator located on the vessel floor directly below the vent line.

4. The number concentration of aerosols is very low ($\leq 10^9$ particle/m^3).

5. The flow is strictly two-dimensional, i.e., end effects are ignored.

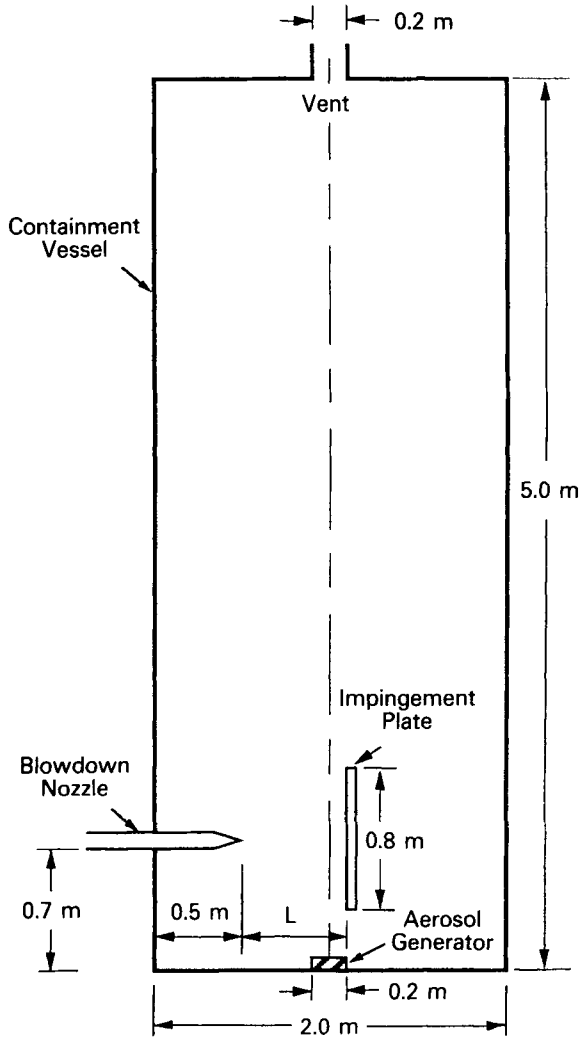

Fig. 1. Containment model used in simulation.

As a corollary to the above assumptions, physical processes influencing aerosol dynamics such as thermophoresis, diffusiophoresis, and coagulation and steam condensation/evaporation can be ignored. Depletion of aerosols on contact with vessel surfaces is also ignored. Therefore, the major aerosol processes modeled are convection and diffusion.

The cases simulated in this study are given in Table II. Three separation distances between the nozzle and the impingement plate were used. The aerosol size and density were varied to investigate their effects on leakage rate through the vent. The aerosol number concentration at the generator was set at 10^8 particle/m^3 except in case E where a tenfold increase was used. Cases A, C, and O are reference cases to study the dynamics of the steam jet in the vessel.

RESULTS AND DISCUSSIONS

The simulations were performed by discharging saturated steam into the steam-filled vessel at a constant velocity of 65 m/s. Adiabatic no-slip conditions were applied to the vessel surfaces. Transients up to 10 s were obtained with time steps

TABLE II

Summary of Physical Parameters Varied

Case	Plate Separation (m)	Steam Flow Rate[a] (kg/s)	Nozzle Height (m)	Aerosol Particle Radius (μm)	Aerosol Particle Density (kg/m^3)	Initial Concentration (particle/m^3)
A	0.04	0.025	0.065	---	---	---
B	0.04	0.025	0.065	5	960	10^8
C	0.37	0.112	0.287	---	---	---
D	0.37	0.112	0.287	5	960	10^8
E	0.37	0.112	0.287	5	960	10^9
F	0.37	0.112	0.287	5	650	10^8
G	0.37	0.112	0.287	5	1125	10^8
H	0.37	0.112	0.287	5	2250	10^8
I	0.37	0.112	0.287	5	4500	10^8
J	0.37	0.112	0.287	5	9000	10^8
K	0.37	0.112	0.287	4	960	10^8
L	0.37	0.112	0.287	6	960	10^8
M	0.37	0.112	0.287	13	960	10^8
N	0.37	0.112	0.287	50	960	10^8
O	1.44	0.112	0.287	---	---	---
P	1.44	0.112	0.287	5	960	10^8

[a]Per metre of containment depth.

<0.5 ms. Note that the flow field inside the vessel is well developed in 10 s. However, it may take much longer for the aerosol concentration to achieve steady state. Therefore, the aerosol results presented below are for comparison purposes only. The qualitative data trends obtained by varying the aerosol size and density are also presented.

Steam Flow Characteristics

The flow fields in the vessel due to the steam jet were first computed as reference cases. They are shown in Fig. 2 for the three impingement plate separation distances used (cases A, C, and O in Table I). Details of the flow field are strongly dependent on the location of the impingement plate. In general, when the steam jet impacts against the plate, the jet splits into two flow streams. The split is more even when the plate is closer to the nozzle. The upward deflected jet then moves toward the vent. The flow field in the upper region of the vessel is very different for the three cases considered. When the impingement plate is almost directly underneath the vent, the upward deflected jet travels almost straight toward the vent (Fig. 2b). When the plate is farthest away from the nozzle, most of the jet is deflected upward, resulting in a strong recirculating vortex (Fig. 2c).

The downward deflected portion of the jet, on the other hand, sets up smaller vortices in front and behind the impingement plate. Details of the flow vortices below the nozzle are again dependent on the plate separations.

Aerosol Flow Characteristics

The dynamic behavior of an aerosol in the reference case flow fields was investigated by introducing an aerosol of specified radius and density into each of the flow fields. The aerosol was introduced by a generator located at the center of the vessel floor and was modeled numerically by specifying the aerosol number concentration as a boundary condition.

The aerosol was assumed to be picked up, carried along, and distributed by the steam flow. The aerosol velocities are thus dependent only on the local steam flow rates and the size and density of aerosol [Eqs. (9) and (10)].

The effects of the separation distance between the impingement plate and the nozzle on aerosol flows are shown in Figs. 3 and 4. The aerosol was assumed to be monodisperse and spherical with a 5-μm diam and a 960 kg/m^3 density (cases B, D, and P in Table II). The density corresponds to that of saturated water at atmospheric pressure.

Figure 3 gives the aerosol flow fields for the three separation distances used. The corresponding steam flow fields shown in Fig. 2 are almost identical. The flow velocities, however, are lower for the aerosol. This is evident by the lower velocities used to normalize the velocity vectors in Fig. 3. The results are expected because the aerosol was transported by the steam flow. The difference between the steam and aerosol velocities (slip velocity) was found to increase as the size and/or density of the aerosol increased.

Figure 4 shows the aerosol concentration distribution (isoconcentration lines) in the vessel for the three impingement plate locations. The lines are defined with respect to the aerosol generator concentration, which was designated 100%. Very different aerosol distributions were obtained. In general, when the impingement plate was closer to the nozzle, the steam flow along the vessel floor tended to be higher (see Fig. 2a); thus, more aerosol was transported by the flow and dispersed to the upper region of the vessel. For the largest separation distance used (1.44 m), a vortex was formed below the jet and in front of the plate (see Fig. 2c). Since the aerosol generator was also located in front of the impingement

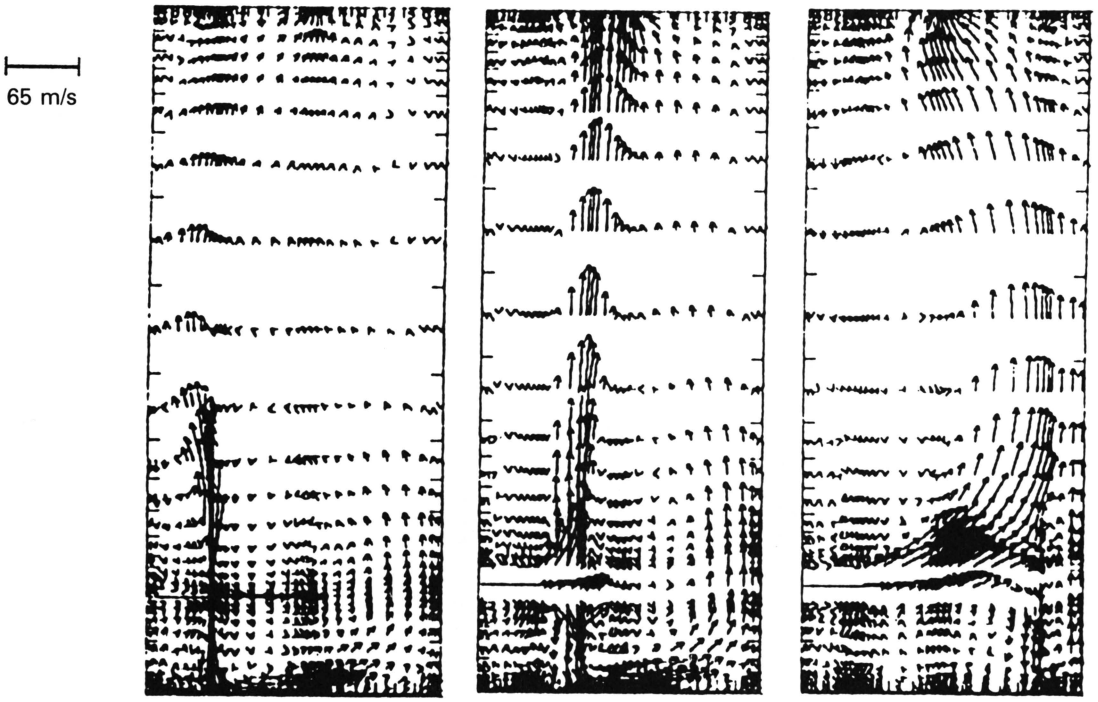

Fig. 2. Steam flow fields.

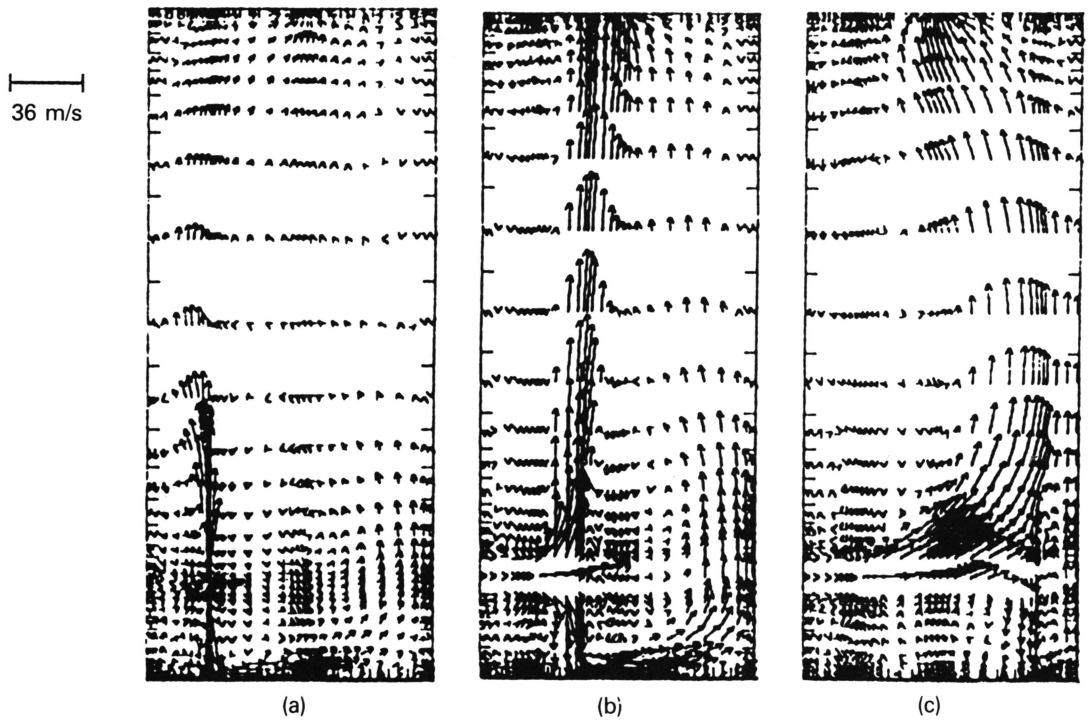

Fig. 3. Aerosol flow fields.

plate, the aerosol was trapped by the resulting vortex. Less aerosol was thus transported upward by the jet.

As discussed above, the aerosol distributions given in Fig. 4 may not be well developed. Therefore, only qualitative comparisons are possible. However, it is clear that the location of the impingement plate is important in determining the aerosol flow characteristics and consequently the aerosol leakage rate through the vent.

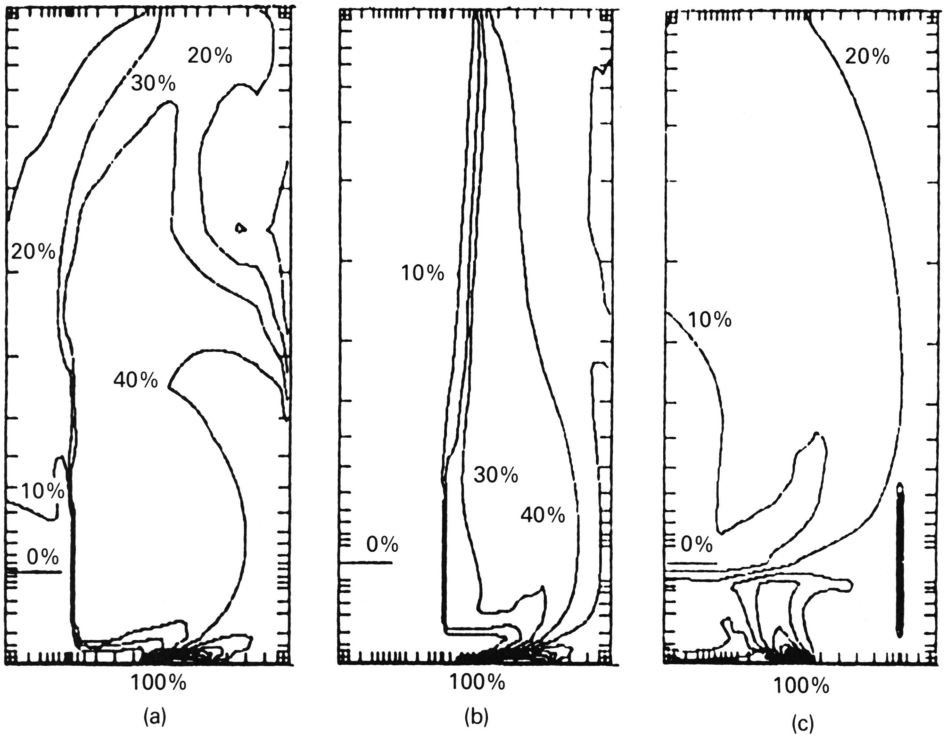

Fig. 4. Aerosol concentration distribution.

Effects of Aerosol Size and Density on Aerosol Distribution

The effect of aerosol size on the leakage rate through the vent (defined as average concentration at vent as percentage of source concentration) is shown in Fig. 5. In this figure, the plate separation was 0.37 m and the density was held constant at 960 kg/m^3 (water droplets). The aerosol radius was varied from 4 to 50 μm. The figure shows that the leakage rate decreases exponentially with increasing aerosol radius.

The results are expected, because for a given aerosol density, the resultant force acting on the aerosol by the carrier gas is inversely proportional to its radius. The ability of the steam to transport the aerosol to the upper portions of the vessel is thus restricted as the aerosol radius increases. Consequently, the aerosol tends to accumulate more and more near the bottom of the vessel.

The effect of aerosol density on leakage rate through the vent is shown in Fig. 6. The plate separation was 0.37 m, and the aerosol radius was held constant at 5 μm. Aerosol density was varied from 650 to 9000 kg/m^3. In this case as well, the aerosol leakage rate decreases exponentially with increasing density owing to the inability of the steam to transport the heavier aerosol to the upper regions of the vessel.

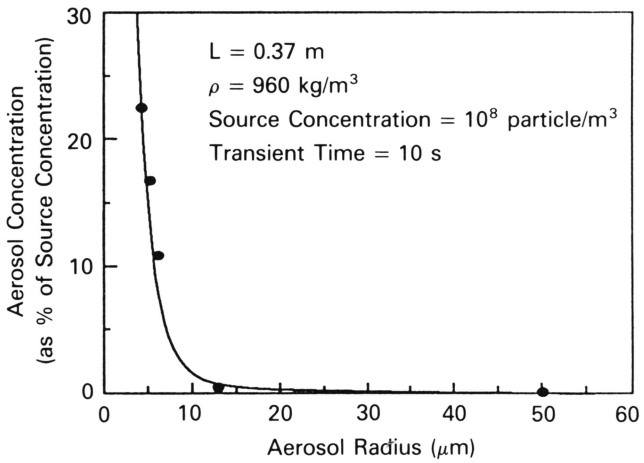

Fig. 5. Graph of average concentration at vent versus aerosol radius.

CONCLUSIONS

The flow of aerosol in a vented containment during a blowdown was simulated numerically. An approach in which the local carrier gas thermal hydraulics and the aerosol dynamics were simultaneously calculated was used. The flow behavior in the containment was modeled using a grid of 32 × 30 cells. The numerical technique used was explicit, and computation was performed using a microcomputer.

The carrier gas and aerosol flow characteristics were investigated systematically for low aerosol number densities. It was found that an obstruction to the jet, which was modeled as an impingement plate, strongly affected the flow characteristics and consequently the aerosol distribution in the vessel and leakage through the vent. The transportation and dispersion of aerosols in the containment by the carrier gas were found to be strongly dependent on the aerosol size and density. In general, a smaller and less dense aerosol followed the gas flow better. For given carrier gas flow conditions, the aerosol concentration at the vent tended to decrease rapidly as the aerosol size or density increased.

Due to the lack of relevant experimental data, no attempt has been made to fine tune or verify the computer code in this

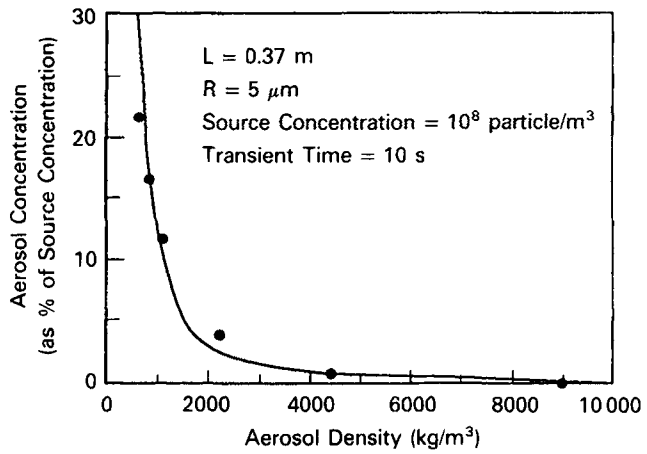

Fig. 6. Graph of average concentration at vent versus aerosol density.

phase of the work. However, results obtained are consistent with physics and physical expectations. The approach used in the present study thus appears to be credible. Code verification will be performed in the future when data become available from experiments being planned.

Efforts are currently being made to incorporate a second aerosol group into the code. Other physical processes such as the flashing jet and the thermophoresis, diffusiophoresis, and coagulation and steam condensation/evaporation of water droplets or aerosols will also be incorporated at later stages.

NOMENCLATURE

C = mean concentration (particle/m^3)

C_1, C_2 = empirical turbulence model constants

C_P = specific heat at constant pressure (J/kg·K)

C_R = reference concentration (particle/m^3)

C_μ = empirical turbulence model constant

D_L, D_T = laminar and turbulent mass diffusivity, respectively (m^2/s)

g = acceleration due to gravity (m/s)

k = turbulent kinetic energy (m^2/s^2)

L = distance between nozzle and impingement plate (m)

Pr_L, Pr_T = laminar and turbulent Prandtl number, respectively (dimensionless)

p' = fluctuation of mean pressure due to natural convection (kg/m·s^2)

R = particle radius (m)

Sc_L, Sc_T = laminar and turbulent Schmidt number, respectively (dimensionless)

T = mean temperature (K)

T_R = reference temperature (K)

t = time (s)

u, U_p = mean gas and particle velocity component in x direction, respectively (m/s)

v, V_p = mean gas and particle velocity component in y direction, respectively (m/s)

x, y = coordinate directions (m)

Greek

α_L, α_T = laminar and turbulent thermal diffusivity, respectively (m^2/s)

β_C = coefficient of concentration expansion (m^3/particle)

β_T = coefficient of thermal expansion (K^{-1})

γ = thermal conductivity (W/m^2·K)

ϵ = dissipation rate of turbulent kinetic energy (m^2/s^2)

μ_L, μ_T = laminar and turbulent viscosity, respectively (kg/m·s)

ρ, ρ_p = gas and particle density, respectively (kg/m^3)

σ_k = Prandtl-Schmidt number for turbulent kinetic energy (dimensionless)

σ_ϵ = Prandtl-Schmidt number for dissipation rate (dimensionless)

REFERENCES

1. F. BEONIO-BROCCHIERI et al., "Nuclear Aerosol Codes," *Nucl. Technol.*, **81**, 193 (1988).

2. I. H. DUNBAR, J. FERMANDJIAN, and J. GAUVAIN, "The Intercomparison of Aerosol Codes," *Nucl. Technol.*, **82**, 36 (1988).

3. A. M. C. CHAN and S. BANERJEE, "Three Dimensional Analysis of Transient Natural Convection in Rectangular Enclosures," *ASME J. Heat Transfer*, **101**, 114 (1979).

4. A. K. AHLUWALIA and M. SHOUKRI, "Numerical Simulation of Transient Turbulent Buoyant Flows," *Proc. 3rd Int. Conf. Numerical Methods in Thermal Problems*, Seattle, Washington, August 1983, Vol. 3, p. 718, Pineridge Press, New York (1983).

5. A. K. AHLUWALIA and A. M. C. CHAN, "Laminar and Turbulent Heat and Mass Transfer by Natural Convection," *Proc. 6th Int. Conf. Numerical Methods in Laminar and Turbulent Flow*, Swansea, U.K., July 1989, Vol. 6, Part 2, p. 2019, Pineridge Press, New York (1989).

6. G. M. HIDY, *Aerosols: An Industrial and Environmental Science*, Academic Press, Inc., New York (1984).

7. F. H. HARLOW and A. A. AMSDEN, "A Numerical Fluids Method for All Speeds," *J. Comput. Phys.*, Vol. 8 (1971).

8. W. RODI, *Turbulence Models and Their Application in Hydraulics*, International Association for Hydraulic Research, The Netherlands (1980).

A. K. Ahluwalia (MSc, mechanical engineering, University of Surrey, United Kingdom, 1974) is a research engineer in the Thermo-Fluids Laboratory at Ontario Hydro Research Division (OHRD). His research interests include experimental and numerical analysis of reactor fluid flow and heat transfer.

A. M. C. Chan (PhD, nuclear engineering, McMaster University, Canada, 1980) is currently head of the Thermo-Fluids Laboratory at OHRD and is associate professor in the mechanical engineering department at McMaster University. His interests include the areas of reactor thermal hydraulics, two-phase flows, and advanced two-phase flow instrumentation.